Control over dark current densities and cutoff wavelengths of GaAs/AlGaAs QWIP grown by multi-wafer MBE reactor

K. Roodenko[a], K.K. Choi[b] ,K. P. Clark[a], E. D. Fraser[a*], , K. W. Vargason[a], J.-M. Kuo[a], Y.-C. Kao[a], P. R. Pinsukanjana[a]

[a]Intelligent Epitaxy Tech Inc, 1250 E. Collins Blvd, Richardson, TX 75081, USA

[b]Electro-optics and Photonics Division, US Army Research Laboratory, 2800 Powder Mill Road, Adelphi, MD 20783, USA

ABSTRACT

Performance of quantum well infrared photodetector (QWIP) device parameters such as detector cutoff wavelength and the dark current density depend strongly on the quality and the control of the epitaxy material growth. In this work, we report on a methodology to precisely control these critical material parameters for long wavelength infrared (LWIR) GaAs/AlGaAs QWIP epi wafers grown by multi-wafer production Molecular beam epitaxy (MBE). Critical growth parameters such as quantum well (QW) thickness, AlGaAs composition and QW doping level are discussed.

Keywords: QWIP, photodetector, MBE, FTIR, infrared, dark current

1. INTRODUCTION

IR detection and imaging is widely used in the military, scientific, commercial and health-related sectors. The advantages of high uniformity, high yield and low cost make quantum-well infrared photodetectors (QWIP) based on a mature GaAs-based III-V material technology an attractive solution for thermal imager applications in long-wave (LW) infrared (8-14 μm) region. The lattice matched GaAs/Al(x)Ga(1-x)As material system is commonly used in QWIP production [1,2,3]. The structures can be routinely and reproducibly grown by epitaxial techniques such as MBE [4] or metalorganic chemical vapor deposition (MOCVD) [5] on GaAs substrates up to 6" diameter. One of the important advantages of these types of photodetectors is the tunability of the material's intersubband transition energy which can be varied over a wide range and tuned to infrared wavelengths above 3μm. However, in a focal plane array (FPA) configuration, the QWIP epi materials are sensitive only to the vertical electric field polarization of the incident light. Therefore, a more complex optical coupling scheme is necessary to efficiently convert the in-plane electric field of the incident radiation into the vertical electric field component. This requires incorporating more complex device processing schemes at the pixel level to optical coupling elements such as grating, resonant cavity or turning mirror within each pixel of the QWIP FPA. Figure 1 shows two different coupling schemes. In Figure 1(a), the corrugated QWIP (C-QWIP) approach is shown, in which the inclined detector sidewalls are used to redirect light parallel to the QW layers [6]. In this case, the coupling mechanism is not wavelength-sensitive but a thick absorber is required to achieve high quantum efficiency (QE). Figure 1(b) shows resonant QWIP (R-QWIP) approach, in which the photon absorption is enhanced by the resonant cavity and metallic diffractive elements [7]. This approach allows for higher QE in a narrow spectral band with a much thinner absorber region: for instance, absorber region with thickness down to 1μm were reported in ref. [8]. However with this technique, the optical resonance of the patterned device geometry occurs at highly selected wavelengths; therefore a much more precise control over the optical absorption peak wavelength of the QWIP epi materials is required. This is achieved during the MBE growth stage of the multiple quantum-well (MQW) region through the control of the quantum well width (the thickness of GaAs layers) and the barrier height (the composition of the AlGaAs layer) [2] that dictate the intersubband transition energy of the QWIP absorber region.

In this manuscript, we address MBE growth of QWIP detectors with a precise control over the absorption peak wavelength through the control of the Al(x)Ga(1-x)As composition and thickness of GaAs. We discuss the dependency of the dark current on the cutoff wavelength and the doping levels. Benefiting from the well-developed theoretical approaches for the detector material design and from the fine the control over MBE growth parameters, the predicted spectral response and the dark current can be targeted with high precision during the MBE growth stages.

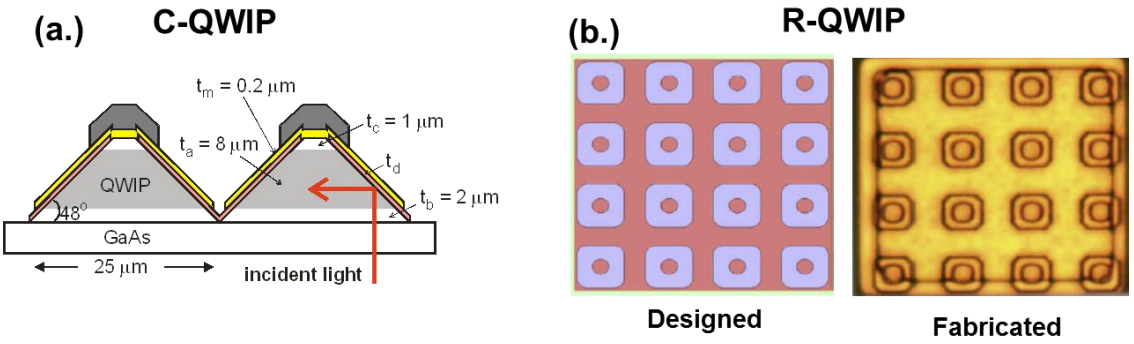

Figure 1. (a) Illustration of the light coupling concept in C-QWIP, after ref. [7]. (b) Illustration of designed and fabricated single-pixel diffractive elements used in R-QWIPs [8].

2. TUNING DETECTOR PARAMETERS DURING MBE GROWTH STAGES

2.1 Experimental

QWIP detectors were grown on semi-insulating GaAs substrates. The production MBE reactors at Intelligent Epitaxy Technology, Inc. (IntelliEPI) used for the QWIP growth are primary used for high volume commercial epi product such as GaAs-based pseudomorphic high electron mobility transistor (PHEMT) for wireless switches, MMIC and automotive radar applications. These multi-wafer MBE reactors are based on the Riber 49, 6000 or 7000 platforms and capable of supporting wafers sizes from 2" to 6". X-ray data were taken by Bede D1 system. For characterization of QWIP detector absorption peak wavelength and the dark current density, the epi materials were processed into large-area devices (LAD) with 1x1 mm^2 square device mesa geometry. The top n-metal contact is an ohmic alloy of Ni:AuGe:Au in grid-pattern. The grip-pattern ohmic contact serves to couple the in-plane electric field component of the incident radiation into perpendicular direction. The Devices with various grid spacing from 60 um to 100 um were fabricated. A piece from an LAD is then mounted and wire bonded to a leadless chip carrier (LCC). Spectral responses were measured at 77K temperature during IR illumination using Nicolet FTIR iS50R spectrometer with each device under bias between the top grid-pattern contact and the bottom ground plane. See Figure 2 for the microscope pictures obtained from the processed devices and the schematic representation of the spectral response measurements.

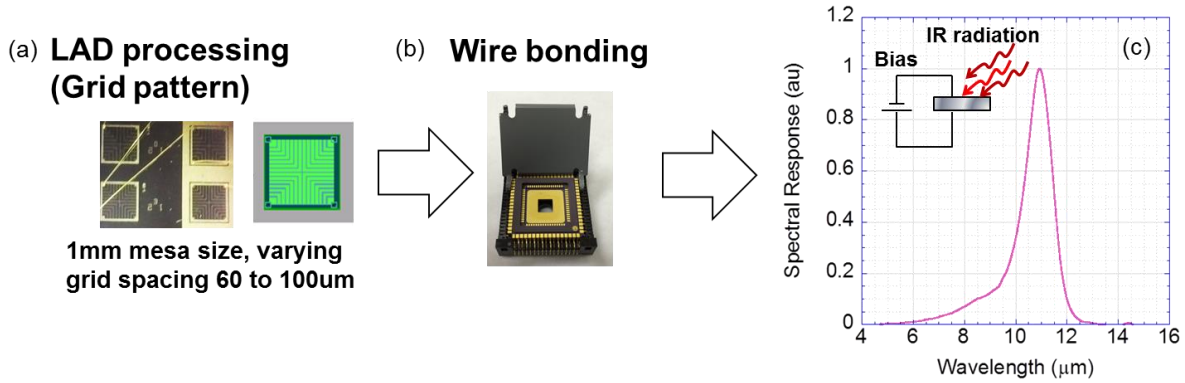

Figure 2. (a) Photograph of wire-bonded devices from a typical QWIP LAD with a grid mask top contact that allows light coupling into GaAs/AlGaAs QWIP material. The scattering mechanism of the light into the QWIP material results in a sufficient signal for testing that is required for fine-tuning of the spectral response peak position. (b) LCC used for wire-bonding and testing of QWIP LAD test pieces. (c) Example of spectral response data with the inset showing a schematic diagram of the light detection for a given device.

2.2 Results and discussion

QWIP absorption peak wavelength is very sensitive to the absorber well thickness and the barrier composition; therefore, a fine control over the growth parameters is required. For FPA applications, it is important to achieve high uniformity of both thickness and composition of these layers across the wafer. Figure 3 shows a set of x-ray data obtained at several positions from a QWIP growth run across GaAs substrates in a Riber 6000 4x6" platen that holds four of 6" diameter wafers. The center of the platen includes a pocket for a quarter of a 4" wafer that can be sacrificed for the subsequent testing. X-ray data indicated layer thickness uniformity of +/- 0.5% across 6" wafer. The stability of the growth rate during the thick absorber structure is indicated by the narrowness of x-ray superlattice peaks. With this 6" QWIP epi material, QmagiQ was able to demonstrate a 320x256 FPA format with 30 um pitch with 100% pixel operability [9].

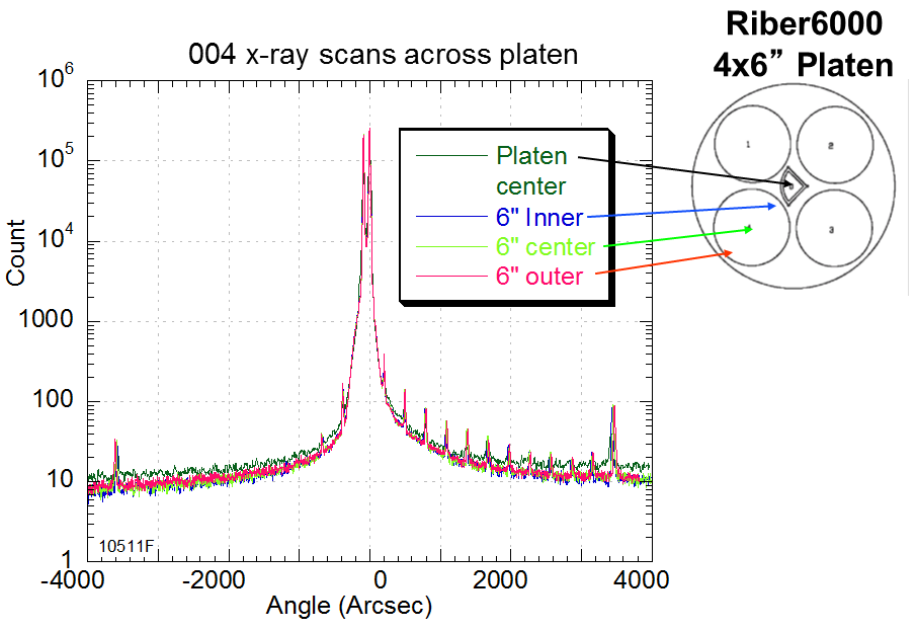

Figure 3. X-ray uniformity data obtained across QWIP wafer grown on a platen holding four of 6" substrates. The thickness uniformity across the wafer was +/- 0.5%. On the inset: illustration of a platen designed to hold four of 6" wafers with a pocket for a quarter of a 4"-diameter wafer at the center.

2.3 Tuning detection wavelength

The control over the detection wavelength can be performed by tuning the quantum well width and the AlGaAs barrier height [2]. Figure 4 shows calibration data (represented by scattered symbols) of the spectral-response peak wavelength dependence on the Al(x)Ga(1-x)As composition for GaAs well thicknesses of 60A, 55A and 50A. The continuous lines were calculated based on the approach described in ref. [2]. For each GaAs well width we find a consistent slope of the peak wavelength vs. AlGaAs composition for all data sets. In practice, this invariability of the slope for various GaAs well thickness (within a specific range [2]) is useful in growth control of the QWIP material, where the growth rates for GaAs wells can be calibrated based on the thick-material growth and then subsequently fine-tune the Al(x)Ga(1-x)As composition to achieve the required detector peak absorption wavelength. It is often the case that the fitting to the X-ray data obtained from the AlGaAs/GaAs superlattice (SL) associated with the QWIP active region is not sensitive enough to small variations in the Al(x)Ga(1-x)As composition which is critical to the positioning of the detection wavelength. Therefore, establishing of the XRD composition calibration curves vs. AlGaAs bandgap based on the growth of the thick AlGaAs material and subsequent photoluminescence/XRD measurements is often required. The possibility to tune growth rates based on the knowledge of the AlGaAs photoluminescence at a given composition enables an easy transfer of the QWIP growth recipe from one MBE campaign to another as well as between the different MBE machines.

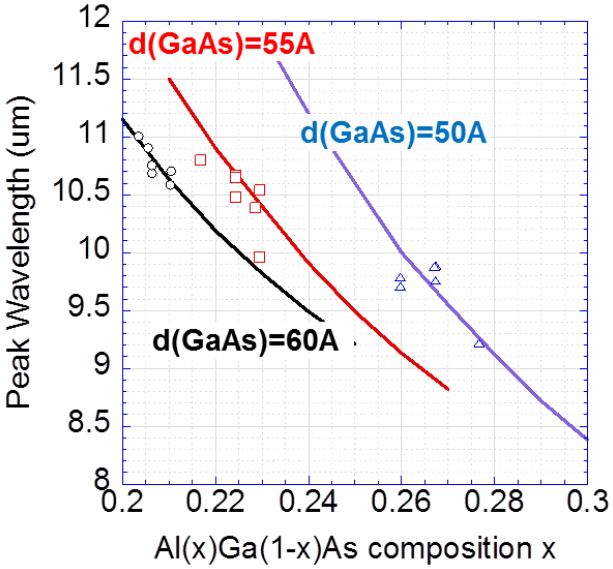

Figure 4. QWIP spectral response peak wavelength as a function of Al(x)Ga(1-x)As composition for GaAs well thickness of 60A (black), 55A (red) and 50A (blue) as obtained from multiple calibration data sets at IntelliEPI. Scattered symbols: measured data; lines: calculated data based on numerical approach in ref. [2]

2.4 Dark current densities

For QWIP devices, there is generally a tradeoff in performance between increasing the quantum efficiency (QE) and decreasing the dark current density. With increasing Si doping concentration of the QWIP active region, both the QE and the dark current density of the device will increase. Therefore, in order for the QWIP devices to achieve optimal performance for each specific application, it is critical to target the dark current density is maintained within the required range. Figure 5(a) shows dark current densities as a function of applied bias for the specified doping densities. Figure 5 (b) shows data of the dark current density (at the 0.02 V normalized to the number of the superlattice periods) as a function of the Si doping level for QWIP detectors with the peak detection wavelength in the range between 10.2 um to 11 um.

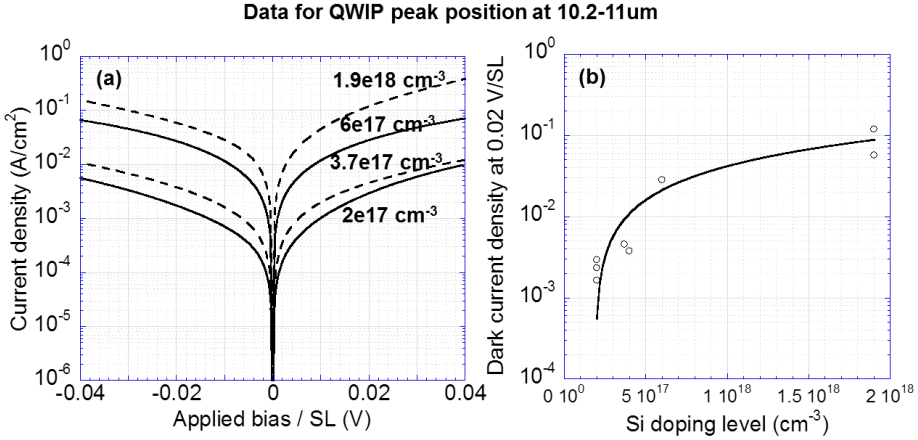

Figure 5. (a) Dark current density as a function of applied bias (bias values are normalized to the number of superlattice periods). The doping levels are indicated on the plots. (b) Dark current density as a function of Si doping levels at the normalized bias per SL period of 0.02V. The data shown is for QWIP devices with the spectral response peak position in the 10.2 – 11 um wavelength range.

In addition to dependence on doping density, the dark current level is dependent on the detector peak detection wavelength. Figure 6 shows dark current density data at T = 77 K obtained from detectors with the active region doped to 1.2e18 cm^{-3}, 6e17 cm^{-3} and 3.7e17cm^{-3} as a function of the peak detection wavelength. The data demonstrates an increase in the dark current density as a function of wavelength with approximately equivalent slopes for each of the doping levels.

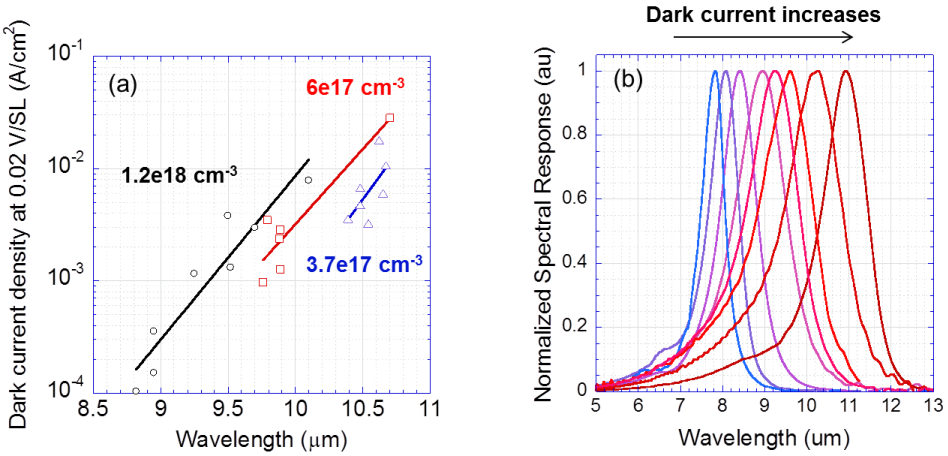

Figure 6. (a) Dark current density at normalized bias of 0.02V/SL as a function of peak detection wavelength. (b) Illustration of the concept of increase in the dark current with the increase in the spectral response peak position.

2.5 Detector growth following a specified design

An implementation of the above considerations during MBE growth stages allows for the control needed for the QWIP epi material to the meet the detection peak wavelength and dark current density requirements. Figure 7 compares the calculated and the measured dark current density (panel (a)) and spectral response (panel (b)) from a LWIR QWIP structure design. The red curves were calculated based on the QWIP epi structure design. The black curves show the measured data from the epi grown QWIP material. The data sets are in a good agreement illustrating the robustness of the theoretical methods behind the QWIP design and the level of control achievable with the QWIP growth on multi-wafer production MBE. This level of control enables one to tune the material growth parameters to reach the specified targets.

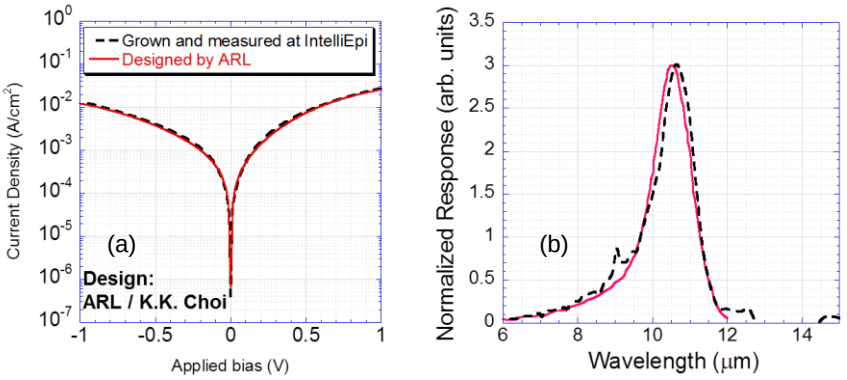

Figure 7. Comparison of the calculated and measured responses for a LWIR QWIP structure design. (a) Designed dark current density (red) and the measured dark current density (black dashed curve) and (b) designed spectral response (red) and measured spectral response (dashed curve). Measurements and targets at T=77K.

2.6 Summary

Recent advances in the R-QWIP design has enabled enhancement in conversion efficiency which in turn leads to shorter integration times applicable to high speed imaging. However, with the resonator structure design which results in higher photon conversion efficiencies at selected wavelength, a more precise control over the peak detection wavelength is required. In this paper we discussed the control of QWIP growths on multi-wafer MBE reactor with high uniformity and reproducibility. Good theoretical understanding of the quantum-well systems and mature electromagnetic models [7] enable the design of QWIP detector material structures that can be realized very close to the expected performance using modern MBE growth technique. An important prerequisite of the reliable and reproducible QWIP growth is the ability to tune spectral response peak position and the dark current densities. Based on the characterization feedback from test structures, the MBE grown QWIP detectors exhibited performance that is true to the designed detector parameters.

REFERENCES

[1] Levine, B. F., "Quantum-well infrared photodetectors", J. Appl. Phys. 74, R1 (1993)

[2] Choi, K. K., "Detection wavelength of quantum-well infrared photodetectors", J. Appl. Phys. 73, 5230 (1993)

[3] Guériaux, V., Brière de l'Isle, N., Berurier, A., Huet, O., Manissadjian, A., Facuetti, H., Marcadet, X., Carras, M., Trinité, V., Nedelcu, A., "Quantum well infrared photodetectors: present and future", Optical Engineering. 50, 061013 (2011)

[4] Fastenau, J. M., Liu, W. K., Fang, X. M., Lubyshev, D. I., Pelzel, R. I., Yurasits, T. R., Stewart, T. R., Lee, J. H., Li, S. S., Tidrow, M. Z., "Commercial production of QWIP wafers by molecular beam epitaxy", Infrared Phys. Technol. 42, 407 (2001)

[5] Martijn, H., Camfeldt, A., Asplund, C., Smuk, S., Kataria, H., Costard, E. "QWIPs at IRnova, a status update", Proc. SPIE 9819, 981918 (2016)

[6] Choi, K. K., Lin, C. H., Leung, K. M., Tamir, T., Mao, J., Tsui, D. C., Jhabvala, M., "Broadband and narrow band light coupling for QWIPs", Infrared Phys. Technol. 44, 309 (2003)

[7] Choi, K. K., Jhabvala, M. D., Forrai, D. P., Waczynski, A., Sun, J., Jones, R., "Electromagnetic modelling of QWIP FPA pixels", Proc. SPIE 8012, 80120R-1 (2011)

[8] DeCuir Jr., E. A., Choi, K. K., Sun, J., Wijewarnasuriya, S., "Progress in resonator quantum well infrared photodetector (R-QWIP) focal plane arrays", Infrared Phys. Technol. 70, 138 (2015)

[9] Reisinger A., Dennis R., Patnaude K., Burrows D., Bundas J., Beech K., Faska R., Sundaram M., "Broadband QWIP FPA for hyperspectral applications", Infrared Phys. Technol. 59, 112 (2013)